Inorg. Chem. **2005**, *44*, 1740–1751

Mono-, Di-, and Tricoordinated Phosphorus Attached to a N–N Unit: An Experimental and Theoretical Study†

Gerd Fischer, Sebastian Herler, Peter Mayer,‡ Axel Schulz,* Alexander Villinger, and Jan J. Weigand

Department of Chemistry and Biochemistry, Ludwig-Maximilians-Universität München Butenandtstrasse 5-13 (Haus F), 81377 München, Germany

Received December 7, 2004

N,*N*′,*N*′-[Tris(trimethylsilyl)]hydrazino-diphenylphosphane, $(TMS)_2N–(TMS)N–PPh_2$ (**1**), and *N*,*N*′,*N*′-[tris(trimethylsilyl)]-hydrazino-phenyl(chloro)phosphane, $(TMS)_2N–(TMS)N–P(Cl)Ph_2$ (**2**), were obtained in the reaction of bis-[lithium-tris(trimethylsilyl)hydrazide] with Ph_nPCl_{3-n} ($n = 1, 2$). The structure and bonding of both species are discussed on the basis of experimentally observed (X-ray, Raman, NMR, and MS) and theoretically obtained data (B3LYP/6-31G(d,p), NBO analysis). Oxidation with sulfur and selenium results in the formation of $(TMS)_2N–(TMS)N–P(S)Ph_2$ (**4**), $(TMS)_2N–(TMS)N–P(Se)Ph_2$ (**5**), $(TMS)_2N–(TMS)N–P(S)Ph(Cl)$ (**6**), and $(TMS)_2N–(TMS)N–P(Se)Ph(Cl)$ (**7**). Moreover, the thermal decomposition of *N*,*N*′,*N*′-[tris(trimethylsilyl)]hydrazine-dichlorophosphane, $(TMS)_2N–(TMS)N–PCl_2$ (**3**) and the reaction with magnesium have been investigated. The formation and molecular structure of the novel $MgCl_2(THF)_2 \cdot 2Mg[(TMS)NP(O)_2N(TMS)_2](THF)$ (**8**) salt containing the hitherto unknown $(TMS)NP(O)_2N(TMS)_2^{2-}$ anion are discussed. DFT calculations (B3LYP/6-311+G(3df,2p)//B3LYP/6-31G(d,p)) are used to evaluate the bonding, ground-state structures, and energy landscape for the different isomers of **3**: the thermodynamics and kinetics of the successive elimination of chlorotrimethylsilane (TMS–Cl) resulting in the formation of covalent azide analogues such as TMS–PNN or TMS–NNP.

Introduction

The low-coordination-number chemistry of the group 15 elements (N, P) has been developed extensively in the past thanks to the use of bulky groups.[1] It has been possible to characterize these reactive species because of their kinetic and thermodynamic stabilization by appropriate substitution.

It was not until 1973 that Flick and Niecke were able to prove the existence of a phosphorus(III) compound with the structural feature of a phosphazene, $-P{=}N-$.[2] This first iminophosphane, a phosphazene with phosphorus in coordination number 2, was obtained in the reaction of bis-(trimethylsilyl)amino(difluoro)phosphane with lithium-bis-(trimethylsilyl)amide (eq 1)

$$(Me_3Si)_2N-PF_2 + LiN(SiMe_3)_2 \rightarrow (Me_3Si)_2N-P{=}SiMe_3 + LiF + Me_3Si-F \quad (1)$$

Shortly thereafter, phosphorus−nitrogen compounds with a two-coordinated phosphorus(III) atom represented a well-established group.[3−5] Because of the large number of stable low-coordinated phosphorus−nitrogen compounds, these species can no longer be regarded as exotic among the main group element compounds. This class of P−N compounds

* To whom correspondence should be addressed. E-mail: lex@cup.uni.muenchen.de. Fax: +49-89-218077492. Phone: +49-89-218077772.

† Dedicated to my father Dr. W. Schulz on the occasion of his 70th birthday.

‡ Performed X-ray structure analysis.

(1) (a) *Multiple Bonds and Low Coordination in Phosphorus Chemistry*; Regitz, M., Scherer, O. J., Eds.; G. Thieme Verlag: Stuttgart, Germany, 1990. (b) Weber, L. *Chem. Rev.* **1992**, *92*, 1839. (c) Weber, L. *Chem. Ber.* **1996**, *129*, 367.

(2) Niecke, E.; Flick, W. *Angew. Chem.* **1973**, *85*, 586−587. Niecke, E.; Flick, W. *Angew. Chem., Int. Ed. Engl.* **1973**, *12*, 585−586.

(3) (a) Scherer, O. J.; Kuhn, N. *Angew. Chem.* **1974**, *86*, 899. Scherer, O. J.; Kuhn, N. *Angew. Chem., Int. Ed. Engl.* **1974**, *13*, 811. (b) Niecke, E.; Scherer O. J. *Nachr. Chem. Tech.* **1975**, *23*, 395. (c) Scherer, O. J.; Kuhn, N. *J. Organomet. Chem.* **1974**, *82*, C3. (d) Scherer, O. J.; Kuhn, N. *Chem. Ber.* **1974**, *107*, 2123−2125. (e) Fleming, S.; Lupton, M. K.; Jekot, K. *Inorg. Chem.* **1972**, *11*, 2534. (f) Maryanoff, B. E.; Hutchins, R. O. *J. Org. Chem.* **1972**, *37*, 3475. (g) Thomas, M. G.; Kopp, R. W.; Schultz, C. W.; Parry, R. W. *J. Am. Chem. Soc.* **1974**, *96*, 2646. (h) Nöth, H.; Ullmann, R. *Chem. Ber.* **1976**, *109*, 1942. (i) Scherer, O. J.; Schnabl, G. *Chem. Ber.* **1976**, *109*, 2996. (j) Niecke, E.; Kröher, R. *Angew. Chem.* **1976**, *88*, 758. Niecke, E.; Kröher, R. *Angew. Chem., Int. Ed. Engl.* **1976**, *15*, 692. (k) Thomas, M. G.; Schultz, C. W.; Parry, R. W. *Inorg. Chem.* **1977**, *16*, 994. (l) Charbonnel, Y.; Barrans, J. *Tetrahedron* **1976**, *32*, 2039. (m) Schmidpeter, A.; Luber, J.; Tautz, H. *Angew. Chem.* **1977**, *89*, 554. Schmidpeter, A.; Luber, J.; Tautz, H. *Angew. Chem., Int. Ed. Engl.* **1977**, *16*, 546.

(4) (a) Pohl, S. *Chem. Ber.* **1979**, *112*, 3159−3165. (b) Pohl, S. *Angew. Chem.* **1976**, *21*, 723. Pohl, S. *Angew. Chem., Int. Ed. Engl.* **1976**, *11*, 687−688.

(5) Niecke, E.; Gudat, D. *Angew. Chem.* **1991**, *103*, 251−270. Niecke, E.; Gudat, D. *Angew. Chem., Int. Ed. Engl.* **1991**, *30*, 0, 217−237 and references therein.

10.1021/ic048286m CCC: $30.25
Published on Web 02/10/2005

Scheme 1

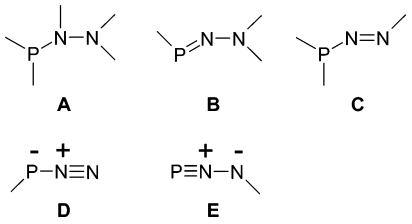

is characterized by large structural diversity and unusual chemical behavior, mainly originating in the (3p−2p)π−P−N bond system representing a highly electronegative fragment including a lone pair.

The synthesis of PN species containing a two-coordinated phosphorus(III) atom such as the iminophosphanes, $R_2N-P{=}NR$, can be achieved by (i) 1.2 elimination,[5] (ii) substitution reaction starting from a known iminophosphane,[6] (iii) conversions[5] for example, by a 1.3 shift of a silyl group,[7] and (iv) ring opening, for example, by thermal treatment of λ^3, λ^5 aza-diphosphiridines.[8] The most convenient synthesis method seems to be the 1.2 elimination of Me_3Si-X from aminophosphanes, which can be generated easily by reaction of PX_3 with lithium amides (eq 2, R = TMS, X = F, Cl, and Br).[3a,5]

$$PX_3 + LiNR_2 \xrightarrow{-LiX} X_2P-NR_2 + LiNR_2 \xrightarrow{-LiX} XP(NR_2)_2 \xrightarrow{\Delta,\,-RX} R_2N-P{=}N-R \quad (2)$$

Much less is known about compounds containing the NNP moiety. With respect to the coordination number at the phosphorus(III) atom, these species can be divided into five classes with a neutral NNP moiety as displayed in Scheme 1. **A** (aminophosphane) and **C** represent tricoordinated phosphorus species or can be regarded as either hydrazine or diazene derivatives. **B** is a phosphinidenehydrazine[9] and represents, in addition to **D**, a dicoordinated phosphorus species. Furthermore, **D** and **E** can be viewed as N- or P-substituted analogues of covalently bound azides. Monocoordinated phosphorus species **E** with a formal NP triple bond can also be considered to be a phosphinidyne derivative.

Hydrazine derivatives of type **A** have been synthesized by Klingebiel et al. in the reaction of bis[lithium-tris-(trimethylsilyl)-hydrazide] with PF_3.[10] When $(TMS)_2N-(TMS)N-PF_2$ was reacted with $LiN(SiMe_3)(CMe_3)$, an unsaturated species of type **B** could be observed. The authors concluded that salt elimination of LiF is followed by the elimination of Me_3SiF, yielding $(TMS)_2N-N{=}P-N(TMS)-(CMe_3)$.

The first structural characterization of a type **B** species was published by Niecke et al. and displayed a rather long P−N bond of 1.598 Å in (tetramethylpiperidino)bis(trimethylsilyl)diazaphosphene. This amino(diaza)phosphene was prepared by treating *N*-(dichlorophosphino)-(2,2,6,6-tetramethyl)piperidine with $LiN(SiMe_3)_2$.[11]

To the best of our knowledge, compounds analogous to covalent azides such as species **D** and **E** (Scheme 1) are not known as well as the all triatomic binary anions composed exclusively of phosphorus and nitrogen atoms and the phosphorus analogue of the azide anion: $N{=}N{=}P^-$, $N{=}P{=}N^-$, $P{=}N{=}P^-$, $P{=}P{=}N^-$, $P{=}P{=}P^-$. The potential energy surfaces of these anions have been calculated using ab initio methods. According to these theoretical results, the N_3^- and N_2P^- ions have linear structures; P_3^- and P_2N^- possess several isomers (linear, bent, or cyclic) close to each other on the energetic scale.[12]

The nature of PN single and double bonds has been extensively studied;[5,13] P−P and P=P bonds are somewhat more elusive.[14] There are only a few examples of compounds containing the N=P−P unit, which is isomeric with P−N−P species. Recently, Dyson et al. showed the reversible rearrangement that is triggered by protonation/deprotonation between diphosphinamines (P−N−P) and iminobiphosphines (N=P−P).[14a]

As part of our research directed toward the synthesis of R−PNN or PNN−R species, we are interested in reactions of the following type

$$\text{(i)}\ R_nPCl_{3-n} + {}^1/_2[LiN(TMS)N(TMS)_2]_2 \xrightarrow{-LiCl} (TMS)_2N-(TMS)N-P(Cl_{2-n})R_n \quad (3)$$

with R = Ph and $n = 0, 1, 2$; (ii) reduction of the $(TMS)_2N-(TMS)N-P(Cl_{2-n})R_n$ ($n = 0, 1$) with magnesium; and (iii) quenching NNP intermediates by the oxidation reaction with oxygen, sulfur, or selenium. In these experiments, we have observed the formation of new compounds such as $(TMS)_2N-$

(6) (a) Scherer, O. J.; Kulbach, N.-T.; Glässel, W. *Z. Naturforsch., B: Anorg. Chem., Org. Chem.* **1978**, *33*, 652. (b) Niecke, E.; Nieger, M.; Reichert, F. *Angew. Chem.* **1988**, *100*, 1781. Niecke, E.; Nieger, M.; Reichert, F. *Angew. Chem., Int. Ed. Engl.* **1988**, *27*, 1715. (c) Romanenko, V. D.; Ruban, A. V.; Markovskii, L. N. *Zh. Obshch. Khim.* **1983**, *53*, 778. (d) Romanenko, V. D.; Ruban, A. V.; Chernega, A. N.; Markovskii, L. N. *Zh. Obshch. Khim.* **1988**, *58*, 2802. (e) Romanenko, V. D.; Ruban, A. V.; Chernega, A. N.; Povolotskii, M. I.; Antipin, Y. M.; Struchkow, Y. T.; Markovskii, L. N. *Zh. Obshch. Khim.* **1988**, *58*, 948. (f) Niecke, E.; Nieger, M.; Gärtner-Winkhaus, C.; Kramer, B. *Chem. Ber.* **1990**, *123*, 477. (g) Niecke, E.; Altmeyer, O.; Barion, D.; Detsch, R.; Gärtner-Winkhaus, C.; Hein, M.; Nieger, M.; Reichert, F. *Phosphorus, Sulfur Silicon Relat. Elem.* **1990**, *49/50*, 321. (h) Niecke, E.; Detsch, R.; Nieger, M. *Chem. Ber.* **1990**, *123*, 797.

(7) Zurmühlen, F.; Regitz, M. *Angew. Chem.* **1987**, *99*, 65. Zurmühlen, F.; Regitz, M. *Angew. Chem., Int. Ed. Engl.* **1987**, *26*, 83.

(8) (a) Niecke, E.; Lysek, M.; Symalla, M. *Chimia* **1986**, *40*, 202. (b) Niecke, E.; Rüger, R.; Schoeller, W. W. *Angew. Chem.* **1981**, *93*, 1110. Niecke, E.; Rüger, R.; Schoeller, W. W. *Angew. Chem., Int. Ed. Engl.* **1981**, *20*, 1034.

(9) David, G.; von der Gonna, V.; Niecke, E.; Busch, T.; Schoeller, W. W.; Rademacher, P. *J. Chem. Soc., Faraday Trans.* **1994**, *90*, 2611−2616.

(10) Bode, K.; Klingebiel, U., Noltemeyer, M.; Witte-Abel, H. *Z. Anorg. Allg. Chem.* **1995**, *621*, 500−505.

(11) Dressler, U.; Niecke, E.; Pohl, S.; Saak, W.; Schoeller, W. W.; Schaefer, H. G. *J. Chem. Soc., Chem. Commun.* **1986**, *14*, 1086−1087.

(12) Chaban, G. M.; Klimenko, N. M.; Charkin, O. P. *Ser. Khim.* **1990**, *7*, 1590−1597. (b) Charkin, O. P.; McKee, M. L.; Schleyer, P. v. R. *Z. Neorgan. Khim.* **1998**, *43*, 280−293.

(13) (a) Burford, N.; Cameron, T. S.; Conroy, K. D.; Ellis, B.; Lumsden, M.; Macdonald, C. L. B.; McDonald, R.; Phillips, A. D.; Ragogna, P. J.; Schurko, R. W.; Walsh, D.; Wasylishen, R. E. *J. Am. Chem. Soc.* **2002**, *124*, 14012. (b) Burford, N.; Cameron, T. S.; LeBlanc, D. J.; Phillips, A. D.; Concolino, T. E.; Lam, K.-C.; Rheingold, A. L. *J. Am. Chem. Soc.* **2000**, *122*, 5413. (c) Burford, N.; Ragogna, P. J.; McDonald, R.; Ferguson, M. J. *Chem. Commun.* **2003**, 2066. (d) Merceron, N.; Miqueu, K.; Baceiredo, A.; Bertrand, G. *J. Am. Chem. Soc.* **2002**, *124*, 6806.

$(TMS)N-P(Cl_{2-n})R_n$ ($m = 1, 2$) together with the previously described species $(TMS)NPN(TMS)_2$[2,3a] under modified reaction conditions. Bis[lithium-tris(trimethylsilyl)-hydrazide] seems to be a good precursor to introduce the NNP moiety via salt elimination, resulting in the formation of tetra-substituted hydrazines.[10,15] The reaction of PCl_3 with $[LiN(TMS)N(TMS)_2]_2$ has already been described by Niecke et al., yielding $(TMS)_2N-(TMS)N-PCl_2$ (**3**).[16]

In this paper, we report (i) our experimental results of the above-mentioned reactions of bis[lithium-tris(trimethylsilyl)-hydrazide][10,15] with R_nPCl_{3-n} and (ii) our theoretical study of the potential energy surface of $(TMS)_2N-(TMS)N-PCl_2$ with respect to the loss of chlorosilane, resulting in the formation of TMS−NNP, $(TMS)_2N-N{=}P-Cl$, and $(TMS)_2$-NPN(TMS) species.

Experimental Section

General Remarks. Solvents were freshly distilled, dried, and stored under nitrogen. NMR: JEOL Eclipse 400 and 270 (^1H, ^{13}C chemical shifts refer to $\delta_{TMS} = 0.00$; ^{31}P refers to $\delta_{H_3PO_4(85\%)} = 0.00$). IR: Nicolet 520 FT-IR (as KBr pellets or in Nujol mulls between KBr windows). Raman: Perkin-Elmer spectrum 2000R NIR FT equipped with a Nd:YAG laser (1064 nm). CHN analyses: Analysator Elementar Vario EL. MS: JEOL MStation JMS 700. Melting points are uncorrected (Büchi B540). Bis[lithium-tris(trimethylsilyl)-hydrazide] was prepared according to the procedure given in the literature.[10,15]

Synthesis of *N,N′,N′*-[Tris(trimethylsilyl)]hydrazino-(diphenyl)phosphane, $(TMS)_2N-(TMS)N-PPh_2$ (1). Into a solution of 1 g (1.95 mmol) of bis[lithium-tris(trimethylsilyl)-hydrazide] in hexane (75 mL), a solution of 0.867 g (3.9 mmol) of freshly distilled $ClPPh_2$ in hexane (25 mL) was added during a period of 1 h at ambient temperature. The white precipitate that was formed (LiCl) was separated by filtration after 2 h. The hexane was removed in vacuum, and a white waxy solid (**1**) was obtained, which still contained traces of LiCl. **1** was purified by sublimation (110 °C, 10^{-3} mbar). $(TMS)_2N-(TMS)N-PPh_2$ (432.76) yield: 1.65 g (98%) colorless crystals, mp 108 °C. IR (KBr, cm^{-1}): $\tilde{\nu}$ 3075 w, 3047 w, 2974 m, 2952 m, 2896 m, 1585 w, 1520 w, 1436 m, 1430 m, 1404 w, 1310 w, 1264 s, 1248 vs, 1242 s, 1179 m, 1104 m, 1085 w, 1067 w, 1030 m, 1014 s, 910 vs, 879 vs, 854 vs, 835 vs, 817 vs, 774 s, 740 s, 705 m, 695 s, 672 s, 618 m, 607 m, 512 m, 487 m, 465 m, 419 w, 385 s, 372 m. Raman (200mW, 25 °C, cm^{-1}): $\tilde{\nu}$ 3172 (0.5), 3138 (0.5), 3055 (9), 2977 (5), 2954 (6), 2899 (10), 1588 (9), 1573 (3), 1410 (2, br), 1180 (2), 1157 (2), 1103 (3), 1089 (3), 1030 (4), 1002 (10), 678 (3), 643 (5), 619 (3), 467 (2), 420 (3), 404 (3), 388 (1), 332 (1), 261 (4), 210 (4). ^1H NMR ($CDCl_3$, 25 °C): δ 0.08 (s, 18 H, TMS), 0.10 (s, 9 H, TMS), 7.32 (m, 4 H, Ph), 7.61 (m, 6 H, Ph). ^{13}C NMR ($CDCl_3$, 25 °C): δ 4.04 (s, $N(Si(\mathbf{C}H_3)_3)_2$), 4.07 (s, $NSi(\mathbf{C}H_3)_3$), 127.94 (d, $^3J_{CP} = 6.2$ Hz, C_{phenyl}), 128.99 (s, br C_{phenyl}), 134.5 (d, $^2J_{CP} = 22.8$ Hz, C_{phenyl}), 140.08 (d, $^1J_{CP} = 20.8$ Hz, C_{phenyl}). ^{31}P NMR ($CDCl_3$, 25 °C): δ 61.4 (s). $^{29}Si\{^1H\}$ NMR ($CDCl_3$, 270 MHz, 25 °C): δ 8.93 (d, $^3J_{SiP} = 1.3$ Hz, $N(\mathbf{Si}(CH_3)_3)_2$), 13.42 (d, $^2J_{SiP} = 7.9$ Hz, $N\mathbf{Si}(CH_3)_3$). MS (EI, 70 eV, >5%) *m*/*z* (%): 432 (3) [M^+], 417 (10) [$M^+ - CH_3$], 332 (6), 331 (20), 321 (8) [$(TMS)_2NN(TMS)_2^+$], 320 (23) [$((TMS)_2NN(TMS)_2 - H)^+$], 305 (7) [$((TMS)_2NN(TMS)_2 - CH_3)^+$], 273 (8) [$(TMS)HN-PPh_2^+$], 272 (30) [$(TMS)N-PPh_2^+$], 248 (5) [$(TMS)_2N-NH(TMS)^+$], 247 (14) [$(TMS)_2N-N(TMS)^+$], 232 (7), 231 (15), 218 (8), 217 (28), 204 (9), 197 (7), 175 (6), 174 (30), 146 (12) [$TMS-TMS^+$], 135 (15), 131 (7), 130 (22), 74 (9) [$HSi(CH_3)_3^+$], 73 (100) [$SiCH_3)_3^+$], 45 (5). $C_{21}H_{37}N_2P_1Si_3$ (432.76): calcd C 58.28, H 8.62, N 6.47; found C 58.63, H 8.44, N 6.02. HR-MS: $C_{21}H_{37}N_2P_1Si_3$ (432.76) requires $M^+ = 432.2002$; found 432.2002.

Synthesis of *N,N′,N′*-[Tris(trimethylsilyl)]hydrazino-phenyl-(chloro)phosphane, $(TMS)_2N-(TMS)N-P(Cl)Ph$ (2). Into a solution of 1 g (1.95 mmol) of bis[lithium-tris(trimethylsilyl)-hydrazide] in hexane (75 mL), a solution of 0.703 g (3.9 mmol) of freshly distilled Cl_2PPh in hexane (25 mL) was added during a period of 1 h at ambient temperature. The white precipitate that was formed (LiCl) was separated by filtration after 2 h. The hexane was removed in vacuum, and a waxy solid (**2**) was obtained, which still contained traces of LiCl. **2** was purified by sublimation (110 °C, 10^{-3} mbar). $(TMS)_2N-(TMS)N-P(Cl)Ph$ (391.11) yield: 1.45 g (95%) colorless crystals, mp 118 °C. IR (KBr, cm^{-1}): $\tilde{\nu}$ 3059 m, 3057 m, 2955 s, 2900 m, 1586 w, 1479 m, 1434 s, 1405 m, 1307 w, 1251 vs, 1249 vs, 1182 w, 1156 w, 1089 s, 1013 s, 913 br vs, 881 vs, 836 vs, 769 s, 742 vs, 699 vs, 661 s, 619 m, 607 m, 581 m, 500 br m, 465 m, 438 w, 417 w, 387 m. Raman (300 mW, 25 °C, cm^{-1}): $\tilde{\nu}$ 3172 (0.5), 3144 (0.5), 3067 (7), 3048 (3), 2956 (5), 2903 (10), 1587 (4), 1574 (1), 1411 (2), 1183 (1), 1159 (1), 1089 (1), 1029 (3), 1003 (5), 689 (2), 666 (2), 648 (6), 620 (1), 499 (1), 448 (3), 413 (1), 372 (4), 346 (1), 272 (5), 197 (3, br). ^1H NMR ($CDCl_3$, 25 °C): δ 0.01 (s, 9 H, TMS), 0.27 (s, 18 H, TMS), 7.42 (m, 2 H, Ph), 7.95 (m, 3 H, Ph). ^{13}C NMR ($CDCl_3$, 25 °C): δ 3.05 (s, $NSi(\mathbf{C}H_3)_3)_2$), 3.09 (s, $NSi(\mathbf{C}H_3)_3$), 128.1 (d, $^3J_{CP} = 6.1$ Hz, C_{phenyl}), 130.6 (s, C_{phenyl}), 132.6 (d, $^2J_{CP} = 26.1$ Hz, C_{phenyl}), 138.20 (d, $^1J_{CP} = 38.4$ Hz, C_{phenyl}). ^{31}P NMR ($CDCl_3$, 25 °C): δ 145.2 (s). $^{29}Si\{^1H\}$ NMR ($CDCl_3$, 25 °C): δ 11.3 (s, $N(\mathbf{Si}(CH_3)_3)_2$), 19.1 (d, $^2J_{SiP} = 2.0$ Hz, $N\mathbf{Si}(CH_3)_3$). MS (EI, 70 eV, >5%) *m*/*z* (%): 390 (3) [M^+], 375 (6) [$M^+ - CH_3$], 289 (5), 248 (8) [$(TMS)_2N-NH(TMS)^+$], 247 (32) [$(TMS)_2N-N(TMS)^+$], 174 (25), 146 (12) [$TMS-TMS^+$], 135 (9), 131 (7), 130 (12), 74 (9) [$HSi(CH_3)_3^+$], 73 (100) [$SiCH_3)_3^+$], 45 (6), 36 (7). $C_{15}H_{32}Cl_1N_2P_1Si_3$ (391.11): calcd C 46.07, H 8.25, N 7.16; found C 46.47, H 8.66, N 7.36.

Synthesis of *N,N′,N′*-[Tris(trimethylsilyl)]hydrazino-(dichloro)phosphane, $(TMS)_2N-(TMS)N-PCl_2$ (3). 3 was prepared according to the procedure given in the literature.[16] **3** can be purified further by sublimation (65 °C, 10^{-3} mbar). $(TMS)_2N-(TMS)N-PCl_2$ (349.46) yield: 90% colorless ceraceous crystals, mp 114 °C (slow dec). Raman (200mW, 25 °C, cm^{-1}): $\tilde{\nu}$ 2960 (5), 2904 (10), 1411 (2), 687 (2), 658 (2), 645 (7), 585 (1.5), 466 (4), 448 (4), 438 (4), 364 (4), 351 (4), 232 (4, br), 188 (4, br), 144 (2, br). ^1H NMR ($CDCl_3$, 25 °C): δ 0.19 (s, 18 H, TMS), 0.38 (s, 9 H, TMS). ^{13}C NMR ($CDCl_3$, 25 °C): δ 2.46 (s, $NSi(\mathbf{C}H_3)_3)_2$), 2.51 (s, $NSi(\mathbf{C}H_3)_3$). ^{31}P NMR ($CDCl_3$, 25 °C): δ 166.6 (s). $^{29}Si\{^1H\}$ NMR ($CDCl_3$, 25

(14) (a) Fei, Z.; Biricik, N.; Zhao, D.; Scopelliti, R.; Dyson, P. J. *Inorg. Chem.* **2004**, *43*, 2228−2230. (b)Yoshifuji, M.; Shima, I.; Inamoto, N.; Hirotsu, K.; Higuchi, T. *J. Am. Chem. Soc.* **1981**, *103*, 4587. (c) Yoshifuji, M.; Shibayama, K.; Inamoto, N.; Matsushita, T.; Nishimoto, K. *J. Am. Chem. Soc.* **1983**, *105*, 2495. (d) Kaukorat, T.; Neda, I.; Schmutzler, R. *Coord. Chem. Rev.* **1994**, *137*, 53. (e) Burford, N.; Cameron, T. S.; LeBlanc, D. J.; Losier, P.; Sereda, S.; Wu, G. *Organometallics* **1997**, *16*, 4712. (f) Kato, T.; Gornitzka, H.; Baceiredo, A.; Schoeller, W. W.; Bertrand, G. *Science* **2000**, *289*, 754. (g) Kato, T.; Gornitzka, H.; Baceiredo, A.; Schoeller, W. W.; Bertrand, G. *J. Am. Chem. Soc.* **2002**, *124*, 2506.

(15) (a) K. Seppelt, W. Sundermeyer, *Chem. Ber.* **1969**, *102*, 1247−1252. (b) Metzler, N.; Nöth, H.; Sachdev, H. *Angew. Chem.* **1994**, *106*, 1837−1839. Metzler, N.; Nöth, H.; Sachdev, H. *Angew. Chem., Int. Ed. Engl.* **1994**, *17*, 1746−1748.

(16) Niecke, E.; Altmeyer, O.; Nieger, M.; Knoll, F. *Angew. Chem.* **1987**, *99*, 1299−1300. Niecke, E.; Altmeyer, O.; Nieger, M.; Knoll, F. *Angew. Chem., Int. Ed. Engl.* **1987**, *26*, 1257.

Table 1. Crystallographic Data

	1	**2**	**4**	**8**
formula	$C_{21}H_{37}N_2PSi_3$	$C_{15}H_{32}ClN_2PSi_3$	$C_{21}H_{37}N_2PSSi_3$	$C_{34}Cl_2H_{86}Mg_3N_4O_8P_2Si_6$
fw	432.77	391.11	464.83	1053.35
cryst syst	triclinic	monoclinic	monoclinic	monoclinic
space group	$P\bar{1}$	$P2_1/n$	$P2_1/n$	$P2_1/n$
a, Å	9.0109(7)	15.581(1)	8.8653(1)	13.669(3)
b, Å	9.3520(8)	9.2489(8)	37.6480(4)	27.625(6)
c, Å	15.344(1)	16.215(1)	16.0046(2)	15.347(3)
α, deg	84.454(1)	90	90	90
β, deg	85.441(2)	110.908(8)	93.2525(4)	98.47(3)
γ, deg	81.534(2)	90	90	90
V, Å^3	1270.2(2)	2182.8(3)	5333.1(1)	5732(2)
Z	2	4	8	4
ρ_{calcd}, g/cm^{-3}	1.132	1.190	1.158	1.221
μ, mm^{-1}	0.259	0.412	0.326	0.371
$\lambda_{Mo\ K\alpha}$, Å	0.71073	0.71073	0.71073	0.71073
T, K	193	200	200	200
reflns collected	5442	10197	43715	83838
independent reflns	2807	2838	7350	13116
R_{int}	0.019	0.094	0.081	0.097
obsd reflns	2451	1573	4734	9196
F(000)	468	840	2000	2264
R_1[a]	0.0375	0.0394	0.0476	0.0509
wR_2[b]	0.1024	0.0802	0.1198	0.1408
GOF	1.044	0.78	1.04	1.04
No. parameters	253	199	505	532
CCDC no.	242754	242755	242756	242757

[a] Final R [$F > 2\sigma(F)$]. [b] R indices (all data).

°C): δ 13.7 (d, $^3J_{SiP} = 2.0$ Hz, N(**Si**(CH$_3$)$_3$)$_2$), 19.8 (d, $^2J_{SiP} = 6.9$ Hz, N**Si**(CH$_3$)$_2$). For MS and CHN analytical data, see ref 16.

Synthesis of $MgCl_2(THF)_2$·2 Mg[N(TMS)P(O)$_2$N(TMS)$_2$](THF) (8). Into a solution of 1.747 g (5.00 mmol) of **3** in 100 mL THF, 0.486 g (20.0 mmol) of magnesium splinters was added at 0 °C. The reaction mixture was allowed to warm to ambient temperature after 3 h at 0 °C and was stirred for 70 h. The solution was filtered, and the solvent was removed in vacuum. The remaining orange oil was recrystallized from anhydrous hexane over a period of 14 days. We assume that oxygen was introduced by either THF or during the recrystallization procedure.[17] When we attempted to isolate a sample for elemental analysis, the crystals released solvent molecules, hence the reported data are fairly inaccurate.

$MgCl_2(THF)_2$·2Mg[N(TMS)P(O)$_2$N(TMS)$_2$](THF) (1053.38) yield: ca. 8% colorless blocks, mp none (upon heating, THF liberation). Raman (200 mW, 25 °C, cm^{-1}): $\tilde{\nu}$ 2960 (8), 2900 (10), 1451 (2, br), 1409 (2, br), 1250(2, br), 1038 (2), 923 (2), 892 (1), 880 (1), 670 (3), 629 (4), 437 (3), 242 (3), 224 (3.5). ^{1}H NMR ($CDCl_3$, 25 °C): δ 0.48 (s, 3 H, Si(C**H**$_3$)$_3$), 1.34 (s, 1 H, THF$_{coord.}$), 3.91 (s, 1H, THF$_{coord.}$). ^{13}C NMR ($CDCl_3$, 25 °C): δ 6.1 (s, Si-(**C**H$_3$)$_3$), 24.9 (THF$_{coord.}$), 69.7 (THF$_{coord.}$). ^{31}P NMR ($CDCl_3$, 25 °C): δ 9.5 (s, br, (TMS)$_2$N**P**(O)$_2$N(TMS)$^{2-}$). ^{29}Si{^{1}H} NMR ($CDCl_3$, 25 °C):δ −7.1 (s). MS (FAB$^-$, xenon, 6keV, m-NBA matrix): 311 [M$_{anion}$ + H$^+$]$^-$, 239 [M$_{anion}$ + 2H$^+$ − TMS$^+$]$^-$. C_{34}-$Cl_2H_{86}Mg_3N_4O_8P_2Si_6$ (1053.38): calcd C 38.77, H 8.23, N 5.32; found C 25.51, H 6.25, N 6.32.

X-ray Analyses. X-ray quality crystals of **1**, **2**, and **4** were obtained by sublimation (see Experimental Section). X-ray quality crystals of **8** were obtained from a yellow hexane/THF solution of **8** after the stepwise removal of solvent. Data for compound **1** were collected on a Siemens CCD area detector using Mo Kα radiation (CCDC 242754), data for **2** were collected on a STOE IPDS (CCDC 242755), and the data for **4** (CCDC 242756) and **8** (CCDC 242757) were collected on a Nonius Kappa CCD, Mo Kα. Crytallographic data are summarized in Table 1. Selected bond lengths and angles are available in Tables S1−S4 (Supporting Information). All of the structures were solved by direct methods (the structure solution program for **1** was SHELXS-97, and SIR97[18] was used for **2**−**4**) and refined by full-matrix least-squares methods with SHELXL-97.[19] Hydrogen atoms were included at geometrically idealized positions and were not refined; the non-hydrogen atoms were refined anisotropically.

Computational Details. Our goal was to compare the structures and energetics of different NNP species attached to 3−1 trimethylsilyl groups. Therefore, it was important to carry out the calculations in such a way that the results could be compared reliably with each other. The structural and vibrational data of all of the considered species were calculated by using hybrid density functional theory (B3LYP) with the program package Gaussian 98.[20] We ran two sets of computations: (i) for all elements, a standard 6-31G(d,p) basis set was used, and (ii) a 6-311+G(3df,2p) standard basis set was applied only for those species with only one TMS group.

Comparison of these data sets shows differences in bond lengths no larger than 0.01−0.02 Å. The bond angles in all of these

(17) Kessenich, E.; Polborn, K.; Schulz, A. *Z. Anorg. Allg. Chem.* **2001**, *627*, 2506−2510.

(18) Altomare, A.; Burla, M. C.; Camalli, M.; Cascarano, G. L.; Giacorazzo, C. *J. Appl. Crystallogr.* **1999**, *32*, 115−119.

(19) Sheldrick, G. M. *SHELXL-97*: *Program for Solution of Crystal Structures*; University of Göttingen: Göttingen, Germany, 1997.

(20) Frisch, M. J.; Trucks, G. W.; Schlegel, H. B.; Scuseria, G. E.; Robb, M. A.; Cheeseman, J. R.; Zakrzewski, V. G.; Montgomery, J. A., Jr.; Stratmann, R. E.; Burant, J. C.; Dapprich, S.; Millam, J. M.; Daniels, A. D.; Kudin, K. N.; Strain, M. C.; Farkas, O.; Tomasi, J.; Barone, V.; Cossi, M.; Cammi, R.; Mennucci, B.; Pomelli, C.; Adamo, C.; Clifford, S.; Ochterski, J.; Petersson, G. A.; Ayala, P. Y.; Cui, Q.; Morokuma, K.; Malick, D. K.; Rabuck, A. D.; Raghavachari, K.; Foresman, J. B.; Cioslowski, J.; Ortiz, J. V.; Stefanov, B. B.; Liu, G.; Liashenko, A.; Piskorz, P.; Komaromi, I.; Gomperts, R.; Martin, R. L.; Fox, D. J.; Keith, T.; Al-Laham, M. A.; Peng, C. Y.; Nanayakkara, A.; Gonzalez, C.; Challacombe, M.; Gill, P. M. W.; Johnson, B. G.; Chen, W.; Wong, M. W.; Andres, J. L.; Head-Gordon, M.; Replogle, E. S.; Pople, J. A. *Gaussian 98*, revisions A7 and A11; Gaussian, Inc.: Pittsburgh, PA, 1998.

molecules are rather constant and relatively independent of the basis sets. Finally, to save CPU time and to obtain a consistent set of data, we decided to use a 6-31G(d,p) basis for all of the molecules.[21]

All of the stationary points were characterized by frequency analysis at the B3LYP level. To obtain more reliable energies and to check the quality of the smaller 6-31G(d,p) basis set, we calculated single points for all of the species by using the optimized B3LYP/6-31G(d,p) structure and the larger 6-311+G(3df,2p) basis set, notation B3LYP/6-311+G(3df,2p))//B3LYP/6-31G(d). The mean deviation for the energies utilizing both basis sets is reasonably small at 2.7 kcal/mol.

NBO analyses[22] were carried out to investigate the bonding in all of the molecules at the SCF level by utilizing the optimized B3LYP/6-31G(d,p) geometry. Furthermore, NBO population analysis for **1** and **2** was carried out with the structure fixed at that determined by X-ray analysis of **1** and **2** to investigate the bonding and hybridization in this experimentally observed species (single point at the HF level).

The search for transition states was usually started with scans along an estimated reaction coordinate. Once a transition state was located, we carried out intrinsic reaction coordinate (IRC) calculations to check whether the located transition states belong to either of the two minima under consideration. Two hundred points in both directions were calculated. In cases in which 200 steps did not lead to a minimum, an optimization followed that utilized the last geometry of the IRC.

Because of the existence of several methyl groups in all of the species, we also had to study the conformational space. In case we were able to find rotamers that are very close in energy, we have calculated the weight factors according to the Boltzmann approach.

The computed geometrical parameters for all of the molecules are given as Supporting Information in Tables S5 and S6, and the relative energies are given in Table 2. Details of the NBO analyses are summarized in Table 3. The computed frequencies and absolute energies are given in the Supporting Information; the IRCs can be obtained from the authors. Molecular models and the numbering of atoms are shown in Figures 1, 6, and 9−12. In our discussion, unless otherwise noted, B3LYP/6-31G(d,p) geometries and energies will be quoted.

It should be emphasized that the computation was carried out for a single, isolated (gas-phase) molecule. There may be significant differences among gas-phase, solution, and solid-state data.

Results and Discussion

Reaction of Ph_2PCl, $PhPCl_2$, and PCl_3 with $[LiN(TMS)N(TMS)_2]_2$. The salt-elimination reaction of di(chloro)phenylphosphane chloride with bis[lithium-tris(trimethylsilyl)-hydrazide] in hexane at ambient temperature represents a fast and clean reaction (reaction time 1 h, yield > 90%), resulting in the formation of hydrazino(diphenyl)-phosphane **1**, $(TMS)_2N-(TMS)N-PPh_2$, (eq 3, $n = 2$, TMS = trimethylsilane). The same holds true for the reaction of phenyl(dichloro)phosphane and phosphorus trichloride with lithium hydrazide in ether. However, only the formation of (hydrazino)phenyl(chloro)phosphane **2**, $(TMS)_2N-(TMS)N-P(Cl)Ph$ (eq 3, $n = 1$), and hydrazino(dichloro)phosphane **3**, $(TMS)_2N-(TMS)N-PCl_2$, could be observed. Even upon heating, no further elimination of chlorotrimethylsilane was detected for **2**. Compound **2** is thermally stable up to over 100 °C. **2** and **1** are volatile at this temperature in vacuum.

Table 2. Relative Energies (kcal/mol) of All Considered Species Fully Optimized at B3LYP/6-31G(d)[a]

species	ΔE	ΔE(LB)[b]	ΔH_{298}	ΔG_{298}
3a	0.0	0.0	0.0	0.0
3b	2.3	2.33	2.5	4.0
3_1r	34.6	35.68	34.3	33.5
3_2a + TMS−Cl	−5.3	−3.01	−6.5	−20.6
3_2b + TMS−Cl	16.9	19.84	15.4	0.7
3_2c + TMS−Cl	20.3	23.72	18.8	3.7
3_2d + TMS−Cl[c]	−16.8	−27.2	−17.8	−34.4
3_2e + TMS−Cl[c]	−16.4	−27.3	−17.5	−34.6
3_2r + TMS−Cl	7.4	5.13	5.5	−8.7
3_2r2 + TMS−Cl	14.7	11.7	12.9	−1.7
3_3a + 2TMS−Cl	−1.9	1.75	−4.2	−31.4
3_3b + 2TMS−Cl	27.1	20.13	24.3	−3.8
3_3c + 2TMS−Cl	−3.6	1.47	−6.2	−33.5
3_3r + 2TMS−Cl	41.1	43.70	37.4	10.2
TS1	10.0	9.94	9.4	12.1
TS2a	47.0	47.46	39.4	45.4
TS2b	42.4	44.67	41.6	42.8
TS3 + TMS−Cl	27.9	30.50	25.4	10.6
TS4 + TMS−Cl	33.3	34.47	30.6	16.4
TS5 + TMS−Cl	22.7	24.92	20.3	6.8
TS6 + TMS−Cl	42.2	48.26	40.0	25.7
TS7 + TMS−Cl	49.0	53.02	46.4	32.4
TS8 + TMS−Cl	35.0	38.89	33.0	19.8
TS9	34.6	35.76	33.7	35.5
TS10	47.9	48.68	47.1	48.4
TS11 + TMS−Cl	57.0	54.71	53.9	40.1
TS12 + 2TMS−Cl	63.0	66.66	58.6	31.5
TS13 + 2TMS−Cl	63.2	59.46	58.5	31.4
TS14 + 2TMS−Cl	50.3	53.84	46.8	21.2
TS15 + TMS−Cl	42.1	37.9	39.1	23.3
TS16 + TMS−Cl	42.8	34.3	40.5	24.9
1_an	0.0	0.0	0.0	0.0
2_an	−56.7	−63.8	−56.1	−57.3
TS_an	2.6	1.3	1.5	1.9

[a] ΔE relative (to **3a** or **1_an**) energy at 0 K without zpe correction. [b] LB = large basis set: B3LYP/6-311+G(3df,2p)//B3LYP/6-31G(d,p). [c] Conformational averaging gives $\Delta E = -16.5$, ΔE(LB) = −27.3, and $\Delta G_{298} = -34.4$ kcal/mol.

Table 3. Summary of the NBO Analysis of **1**, **2**, and **3** (Net Charges in *e*, LP(X) → σ^*(YZ) Donor−Acceptor Interactions in kcal/mol)[a−c]

	1	**2**	**3a**	**3b**
Q_P	+1.093	+1.221	1.208	1.175
Q_{N1}	−1.043	−1.119	−1.157	−1.137
Q_{N2}	−1.179	−1.204	−1.244	−1.234
Q_{L1}[a]	−0.372	−0.458	−0.397	−0.400
Q_{L2}[a]	−0.388	−0.412	−0.368	−0.335
sp^λ LP(P), λ =	1.19	0.73	0.45	0.51
σ(PN): $c(P)^2/c(N)^2$ in %	25.7/74.3	22.7/77.3	23.5/76.5	24.1/75.9
LP(N1) → σ^*(PL1)	7	2	23	27
LP(N1) → σ^*(PL2)	6	24	7	6
LP(P1) → σ^*(N1N2)	10	<0.5	<0.5	8
LP(P1) → σ^*(N1Si)	<0.5	9	7	6

[a] For **1**, L1 = L2 = C; for **2**, L1 = C, L2 = Cl; and for **3**, L1 = L2 = Cl. [b] For **1** and **2**, the experimental data have been used in the NBO algorithm, and for **3**, the calculated structural data have been used in the NBO algorithm. [c] LP = lone pair.

(21) Klapötke, T. M.; Schulz, A. *Ab Initio Methods in Main Group Chemistry* (with an invited chapter by R. D. Harcourt about VB Theory); John Wiley & Sons: New York, 1998.

(22) (a) Glendening, E. D.; Reed, A. E.; Carpenter, J. E.; Weinhold, F. *NBO*, version 3.1; (b) Carpenter, J. E.; Weinhold, F. *J. Mol. Struct: THEOCHEM* **1988**, *169*, 41. (c) Foster, J. P.; Weinhold, F. *J. Am. Chem. Soc.* **1980**, *102*, 7211. (d) Reed, A. E.; Weinhold, F. *J. Chem. Phys.* **1983**, *78*, 4066. (e) Reed, A. E.; Weinstock, R. B.; Weinhold, F. *J. Chem. Phys.* **1985**, *83*, 735. (f) Reed, A. E.; Schleyer, P. v. R. *J. Am. Chem. Soc.* **1987**, *109*, 7362. (g) Reed, A. E.; Schleyer, P. v. R. *Inorg. Chem.* **1988**, *27*, 3969. (h) Weinhold, F.; Carpenter, J. E. *The Structure of Small Molecules and Ions*; Plenum Press: New York, 1988; p 227.

Table 4. Selected ^{31}P, $^{29}Si\{H\}$, and ^{13}C NMR Shifts of **1**−**8** and Related Compounds

species	^{31}P	^{29}Si	^{13}C	reference
1	61.4	8.9 ($SiMe_3$)$_2$	4.04	this paper
		13.4 $SiMe_3$	4.07	
2	145.2	11.3 ($SiMe_3$)$_2$	3.05	this paper
		19.2 $SiMe_3$	3.09	
3	166.6	13.7 $SiMe_3$	2.46	this paper
		19.8 ($SiMe_3$)$_2$	2.51	
$(TMS)_2N-(TMS)N-PF_2$	154.8	12.5 ($SiMe_3$)$_2$	1.66	ref 10
		15.1 $SiMe_3$	2.33	
$[(TMS)_2N]_2PCl$	186.0		5.23	ref 31
$[(TMS)_2N]_2P^+AlCl_4^-$	450.3		3.54	ref 31
$(TMS)_2NP(N\text{-}TMS)_2$	55.5	−8.0 =N−$SiMe_3$	3.0	ref 39
		9.4−N($SiMe_3$)$_2$	3.5	
4	66.7	11.6 ($SiMe_3$)$_2$	4.31	this paper
		15.8 $SiMe_3$	4.98	
5	66.3	11.7 ($SiMe_3$)$_2$	4.62	this paper
		16.2 $SiMe_3$	5.29	
6	91.3	12.4 ($SiMe_3$)$_2$	3.89	this paper
		19.5 $SiMe_3$	3.91	
7	84.7	12.6 ($SiMe_3$)$_2$	3.48	this paper
		20.0 $SiMe_3$	3.53	
8	9.5	9.5 ($SiMe_3$)$_2$[a]	6.10[a]	this paper
		9.5 $SiMe_3$	6.10	

[a] Only one resonance was observed because of fast TMS exchange on the NMR time scale[2a].

Hence, both crude products of **1** and **2** are purified easily by sublimation from 100−120 °C and 10^{-3} mbar (separation from traces of LiCl) or by recrystallization from pentane. Both species are air and moisture-sensitive, but under argon they are stable over a long period in both solid and common organic solvents (e.g., THF, CH_2Cl_2, hexane, ether, etc.). The very good solubility in almost all common organic solvents makes both compounds good precursors for further synthesis. Also, **3** can be sublimed easily (65 °C, 10^{-3} mbar), resulting in white ceraceous needles; however, these needles are thermally unstable with respect to TMS−Cl release.

Spectroscopic Characterization of 1−3. The formation of both **1** and **2** was unequivocally confirmed by C, H, N analysis, Raman, IR, and NMR spectroscopy, and X-ray diffraction experiments (see Experimental Section). The ^{31}P, ^{29}Si, and ^{13}C NMR data of both compounds together with data of related species and **3** are summarized in Table 4. The $\delta^{31}P$ values of NNP species **1**−**3** are in the range that was expected on the basis of numerous data from the literature.[5,23] Successive replacement of chlorine at phosphorus by a phenyl group leads to increased ^{31}P nuclear shielding (**3** → **2** $\Delta\delta^{31}P = -21$, **2** → **1** $\Delta\delta^{31}P = -84$).[24] As expected, two resonances were observed in the ^{29}Si NMR experiments of **1**−**3**. The two different Si resonances [Si_1: N(TMS), $Si_{2,3}$: N(TMS)$_2$] of the hydrazine unit are assigned easily with the help of the $^2J(^{29}Si^{31}P)$ and $^3J(^{29}Si^{31}P)$ coupling constants. The resonance signal of the TMS group (Si_1) adjacent to the P atom is always observed at larger $\delta^{29}Si$ values compared to the resonance signal of $Si_{2,3}$, displaying stronger deshielded ^{29}Si nuclei (**1**: $\Delta(Si_1-Si_{2,3})\delta^{29}Si = 4.5$; **2**: $\Delta(Si_1-Si_{2,3})\delta^{29}Si = 7.8$; **3**: $\Delta(Si_1-Si_{2,3})\delta^{29}Si = 6.1$). The $^2J(^{29}Si^{31}P)$ coupling constant is in the range of 2−8 Hz and is always larger than the $^3J(^{29}Si^{31}P)$ coupling constants (<2 Hz, often not observed).[10,16]

The Raman and IR data are not very significant because of the large number of normal modes of the N(TMS)N-(TMS)$_2$ moiety along the whole measurement range between 3000 and 200 cm^{-1} (ν_{NN} ca. 1050 cm^{-1}).[15a,25] Moreover, the positions of the N(TMS)N(TMS)$_2$ normal modes are not very sensitive upon substitution. The P−N stretching mode is observed at roughly 850 cm^{-1} (**1**: 850, **2**: 845, and **3**: 853 cm^{-1}), which was confirmed by DFT frequency data. The P−Cl stretching mode of **2** was found at 372 cm^{-1}, and for **3** it was found at 448 (in-phase) and 364 cm^{-1} (out-of-phase mode).

Structure and Bonding of 1, 2, and 3. Inspection of the conformational space showed two isomers for all three species at the B3LYP/6-31G(d,p) level of theory (Figure 1). The main difference between the two isomers is the position of the two (Cl or phenyl) groups attached to the phosphorus atom, which is either trans (isomer **A**) or cis (isomer **B**) with respect to the N2 atom. Because of steric repulsion in the cis arrangement, a larger N−N−P angle (ca. 127°) is found for isomer **B** compared to that of isomer **A** (107−112°). Both isomers are close in energy (ΔE < 3 kcal/mol, Table S5) and hence can be expected to be experimentally observed because only small lattice effects are necessary to favor the higher-lying isomer. In all three cases, the most stable isomer in the gas phase is species **A**. So far, we have been able to obtain only structural data (X-ray) for **1** (isomer **B**) and **2** (isomer **A**).

1 crystallizes in triclinic space group $P\bar{1}$ with two molecules in the unit cell corresponding to isomer type **B** (Figure 1). The perspective view of **1** is depicted in Figure 2. In agreement with our computation, the molecule adopts a staggered configuration with the two planes (P1−N1−Si1−N2 and N1−N2−Si2−Si3) perpendicular to each other (<P1−N1−N2−Si2 = 89.35°). According to our calculations, the rotation about the P−N1 axis is sterically hindered by ca. 10 kcal/mol. We were not able to freeze out the different isomers on the NMR time scale.

The phosphorus atom sits in a pyramidal environment with bond angles between 103 and 109°. In contrast to the P−C bond lengths (1.822(3), 1.838(3) Å), the experimentally determined P−N bond length of 1.704(2) Å is slightly shorter than expected for a typical P−N single bond (cf. Σr_{cov} 1.80 (1.76) Å).[26,27] The σ-bond system along the P1−N1−N2 unit is highly polarized between P1 and N2 and almost ideally covalent between the adjacent N1−N2 single bond with a bond length of 1.476(3) Å. The calculated natural atomic population (NAO)[22] net charges are $Q_{P1} = +1.09e$ on phosphorus, $Q_{N1} = -1.04e$ on the adjacent nitrogen, and $Q_{N2} = -1.18e$ on the second nitrogen atom (Table 3).

(23) Wrackmeyer, B.; Schiller, J. *Z. Naturforsch.* **1992**, *47B*, 662−667.
(24) Berger, S.; Bock, W.; Frenking, G.; Jonas, V.; Müller, F. *J. Am. Chem. Soc.* **1995**, *117*, 3820−3829.
(25) Seppelt, K.; Eysel, H. *Z. Anorg. Allg. Chem.* **1971**, *384*, 147−154.
(26) The first value corresponds to the sum of covalent radii, $r(P) = 1.1$ and $r(N) = 0.7$; however, bond lengths between two elements with large differences in electronegativity are often corrected according to $d_{AB} = r_A + r_B - c|\chi_A - \chi_B|$ (Schomaker−Steveson equation), Holleman, Wiberg. *Lehrbuch der Anorganischen Chemie*, 101. Aufl., Walter de Gruyter, 1995, Anhang V.
(27) Niecke, E.; Altmeyer, O.; Nieger, M. *J. Chem. Soc., Chem. Commun.* **1988**, 945−946.

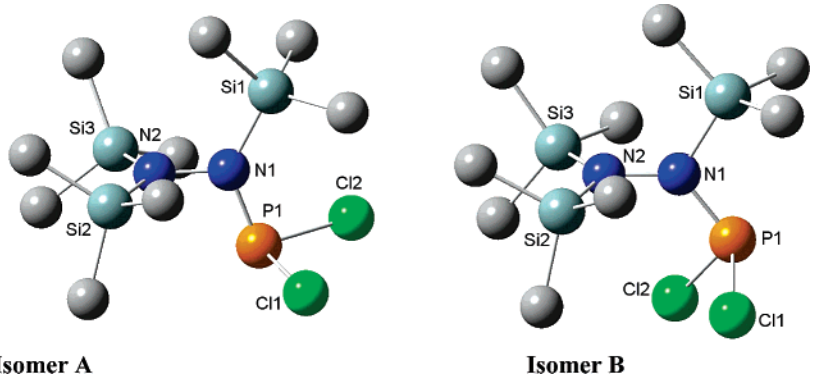

Figure 1. Calculated molecular structure (B3LYP/6-31G(d,p)) of both isomers of **3** (H atoms omitted).

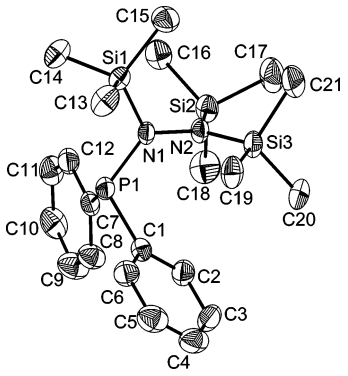

Figure 2. ORTEP drawing of **1**. Thermal ellipsoids with 50% probability at 193 K (hydrogen atoms omitted). Bond lengths [Å] and angles [deg]: P1−N1 1.704(2), P1−C7 1.838(3), P1−C1 1.822(3), N1−N2 1.476(3), Si1−N1 1.768(2), Si2−N2 1.760(2), Si3−N2 1.762(2); N2−N1−P1 126.4-(2), N1−P1−C1 107.6(1), N1−P1−C7 109.2(1), C1−P1−C7 102.9(1), N2−N1−Si1 122.0(2), P1−N1−Si1 111.4(1), N1−N2−Si2 117.1(2), N1−N2−Si3 119.8(2).

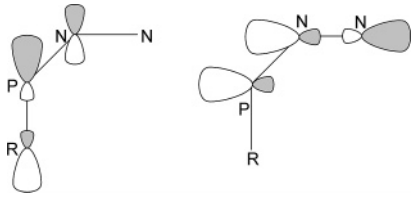

Figure 3. Intramolecular donor−acceptor interactions in **1**−**7**: LP(N) → σ*(PR) and LP(P)→ σ*(NN).

Both nitrogen atoms sit in an almost planar environment (∠Si2−N2−N1−Si3 = 174.9, ∠Si1−N1−P1−N2 = 174.7°; all N−N−X angles are between 117 and 126°, X = P, Si). Hence, as displayed by NBO analysis, the one lone pair on both nitrogen atoms is localized in a pure p-type atomic orbital. Both lone pairs are also perpendicular to each other. As a consequence, the p-type lone pair at the N1 atom (notation: p-LP) is slightly further delocalized, resulting in intramolecular interactions (noncovalent effects). As indicated by an investigation of the noncovalent effects,[22] there are two significant interactions of the N1 lone pair (p-LP) with the two unoccupied, localized antibonding σ*(P−C) orbitals (P1−C7 and P1−C18, Figures 2 and 3). Moreover, the lone pair that is localized at the P atom interacts with the unoccupied σ*(N−N) bond orbital. These intramolecular LP(N) → σ*(P−R) and LP(P)→ σ*(N−N) donor−acceptor interactions (R = C_{phenyl} atom, hyperconjugation ca. 8−13 kcal/mol, Table 3) account for the rather short P−N distance

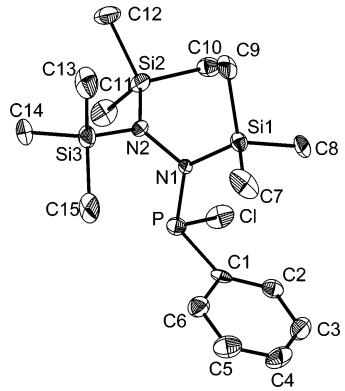

Figure 4. ORTEP drawing of **2**. Thermal ellipsoids with 50% probability at 200 K (hydrogen atoms omitted). Bond lengths [Å] and angles [deg]: P−N1 1.683(3), P−Cl 2.134(2), P−C1 1.840(4), N1−N2 1.473(4), Si1−N1 1.781(3), Si2−N2 1.753(3), Si3−N2 1.767(3); Cl−P−N1 106.4(1), Cl−P−C1 97.5(1), N1−P−C1 103.0(2), P−N1−Si1 132.0(2), P−N1−N2 110.5(2), Si1−N1−N2 117.5(2), Si2−N2−Si3 125.2(2), Si2−N2−N1 118.0(2), Si3−N2−N1 116.6(2).

by introducing a small amount of π interaction (Figure 3). Similar structural features with short P−N distances (1.67 ± 3 Å) have been observed previously in a series of amino-iminophosphanes ($R_2N-P{=}N-R'$).[5]

Compound **2** crystallizes in monoclinic space group $P2_1/n$ with four molecules in the unit cell (Figure 4). In contrast to that of **1**, the molecular structure of **2** corresponds to isomer type **A** (Figure 1). Nevertheless, the molecular structure of **2** strongly resembles the molecular structure of **1**: (i) a staggered conformation with two perpendicular planes was found (dihedral angle: ∠P−N1−N2−Si3 = 88.4°), (ii) both nitrogen atoms are in an ideal planar environment (Σ∠(N1) = 359.95°, Σ∠(N2) = 359.8°), and (iii) a short P−N distance with 1.683(3) Å was found, which is 0.021 Å shorter than the P−N distance in **1**.

Compared to that of **1**, the p-type lone pair of N1 can interact better with the unoccupied σ*(P−Cl) orbital (energy gain of 24 vs 6 kcal/mol, Table 3), resulting in a weakening of the P−Cl bond and a strengthening of the P−N bond. In agreement with this large donor−acceptor interaction, the P−Cl distance is rather long, 2.134(2) Å compared to 2.043-(3) Å in PCl_3, indicating charge transfer into the σ*(P−Cl) bond orbital.[28,29]

(28) Aubauer, C.; Schulz, A.; Klapötke, T. M. *J. Mol. Struct.: THEOCHEM* 2001, *543*, 285−297.
(29) Kisliuk, P.; Townes, C. H. *J. Chem. Phys.* **1950**, *18*, 1109.

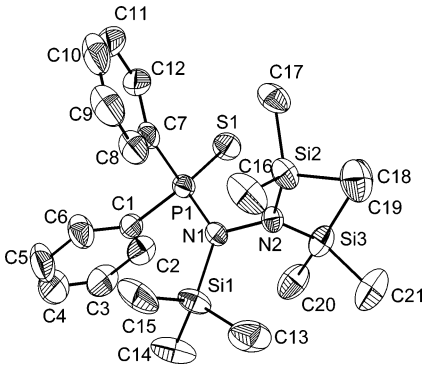

Figure 5. ORTEP drawing of **4**. Thermal ellipsoids with 50% probability at 200 K (hydrogen atoms omitted). Bond lengths [Å] and angles [deg]: S1−P1 1.937(1), P1−N1 1.697(3), P1−C1 1.814(3), P1−C7, N1−N2 1.483(3), Si1−N1 1.790(3), Si2−N2 1.755(3), Si3−N2 1.766(3); S1−P1−N1 115.5(1), S1−P1−C1 111.4(1), N1−P1−C1 105.2(1), P1−N1−N2 114.9(2), P1−N1−Si1 129.2(2), Si1−N1−N2 115.7(2).

To summarize the structure and bonding of compounds **1**−**3**, we can establish the following structural trends: (i) the P−N and N−N distances decrease from **1** to **3** and from isomer **A** to **B** and (ii) the angles do not change much for species **1**−**3**, although the N−N−P angle in all **B** isomers is roughly 17° larger than in isomer **A** (Tables S1−S3, S5). The decreasing P−N and N−N bond lengths can be explained by increasing intramolecular donor−acceptor interaction along the **1**−**3** series, resulting in some π character along the N−P unit. The two different P−Cl bond lengths in **3** nicely correspond to the different magnitude of the p-LP(N) → σ*(P−Cl) donor−acceptor interaction. That is, the larger this type of intramolecular interaction, the larger the P−Cl distance (Tables 3, S6).

Oxidation with Sulfur, Selenium, and Oxygen. 1 can be oxidized easily at ambient temperature with elemental selenium or sulfur, leading to phosphorus(V) species **4**, $(TMS)_2N-(TMS)N-P(S)Ph_2$, and **5**, $(TMS)_2N-(TMS)N-P(Se)Ph_2$, respectively.[3a] In both cases, the white crude products (yield >95%) can be purified by sublimation.

Compound **4** crystallizes in monoclinic space group $P2_1/n$ with eight molecules in the unit cell. The perspective view of the two independent molecules of **4** is shown in Figure 5. The X-ray study of **4** revealed structural features similar to those that were found for **1** and **2**. The compound has distorted trigonal-planar geometry around the central N, and the N−Si and P═S bonds are in trans positions with respect to the N−P bond, which is in agreement with the structural data that was found for dimethyl(thio)[(trimethylsilyl)amino]-phosphorane.[30]

The P−N, N−N, and Si−N bond lengths do not change much upon oxidation (cf. d(P−N) = 1.704(2) (**1**) vs 1.697-(3) Å (**4**)), and the P−S distance of 1.937(1)−1.940(1) Å is slightly elongated (cf. Σr_{cov}(P═S) = 1.91 Å)[26] because of the intramolecular interaction of the p-LP of the N atom with the σ*(P−S) bond (see discussion above, Figure 3).

The analogous oxidation reactions of **2** and **3** with sulfur and selenium are not as straightforward as those of **1**. After 36 h of reflux in THF, ^{31}P NMR and mass spectrometry experiments revealed only small amounts of the oxidized phosphorus(V) species (**6**: $(TMS)_2N-(TMS)N-P(S)Ph(Cl)$, **7**: $(TMS)_2N-(TMS)N-P(Se)Ph(Cl)$), but large amounts of the starting materials were revealed (**6**: 5%, **7**: 20% yield). However, addition of $AlCl_3$ enhances the yield (10−30%, reaction time 3 days) by accelerating the reaction. Cowley et al. have shown that it is not possible to generate cations from R_2NPCl by adding $AlCl_3$ when R = ^{t}BuMe$_3$Si.[31] No chloride ion abstraction occurred, but the formation of a P-bonded Lewis acid−base complex was observed. However, chloride abstraction was observed for R = Me_2N or TMS. We were not able to establish the formation of phosphenium cations in the reaction of **2** with $AlCl_3$ at ambient temperature in ^{31}P NMR experiments.

Upon oxidation, no strong effect on the resonance signal could be observed in the ^{31}P experiments of the oxidized species of **1** (**4** and **5**, Table 4; **1** → **4** $\Delta\delta^{31}$P = 5.3, **1** → **5** $\Delta\delta^{31}$P = 4.9), whereas large $\Delta\delta^{31}$P values of −53.9 and −60.5 were observed for the oxidation products of **2** (**6** and **7**). Moreover, replacing chlorine with a phenyl group yields a shielding effect.

The oxidation of **3** did not succeed. Because **3** is thermally labile with respect to slow liberation of TMS−Cl, several products were observed in the ^{31}P NMR thermolysis experiments that had a longer reaction time. When the reaction is carried out without oxidizer (THF reflux, argon), a decrease of the intensity of the resonance signal of the starting material is observed, whereas only one new resonance signal is observed after 3 h at 485 ppm. At the same time, a white residue has been formed. This reaction can be accelerated by adding small amounts of $AlCl_3$; however, after 6 h of reflux, the resonance signal at 485 ppm vanishes, and no further resonance signal could be observed in the ^{31}P experiment.

Finally, we have tried to react **3** with elemental magnesium in THF under reflux conditions. ^{31}P NMR studies revealed a resonance signal at 130 ppm and a series of resonance signals in the range from 300−370 ppm, of which the resonance with the largest intensity at 326 ppm could be assigned to (TMS)NPN(TMS).[2,3b,32] With increasing reaction time, resonance signals of oxidation products in the range from 0 to −10 ppm were observed, of which the resonance at −9 ppm could be assigned to the $[(TMS)NP(O)_2N-(TMS)]^{2-}$ anion later. Removal of THF after 24 h and recrystallization from a THF/hexane mixture led to a white crystalline species. Single-crystal X-ray studies in combination with ^{31}P NMR, Raman, and mass spectrometry experiments revealed the formation of a $MgCl_2(THF)_2$·2Mg[(TMS)-$NP(O)_2N(TMS)_2$](THF) double salt (**8**). Presumably, oxygen has been introduced during the reflux process. It is interesting that we were able to detect the $[[N(TMS)P(O)_2N(TMS)_2]^{2-} + H^+]$ anion in a FAB^- mass spectrometry experiment that was carried out with crystals of **8**.

(30) Hosmane, N. S.; Arif, A. M.; Cowley, A. H. *Acta Crystallogr., Sect. C* **1987**, *43* (10), 2013−15.

(31) Cowley, A. H.; Lattman, M.; Wilburn, J. C. *Inorg. Chem.* **1981**, *20*, 2916−2919.

(32) Scherer, O. J.; Glässel, W. *Chem. Ber.* **1977**, *110*, 3874−3888.

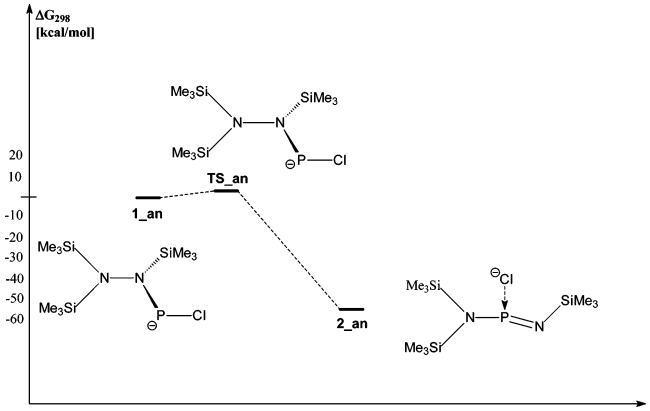

Figure 6. PES for the rearrangement of the NNP to a NPN moiety (B3LYP/6-31G(d,p)).

Because the formation of (TMS)NPN(TMS) could be established by ^{31}P NMR studies, we assume that the following reaction sequence may have occurred, resulting in the formation of **8** (eq 4):

$$(TMS)_2N-(TMS)N-PCl_2 + Mg + 2THF \rightarrow (TMS)_2N-P{=}N(TMS) + MgCl_2(THF)_2 \quad (4)$$

$$(TMS)_2N-P{=}N(TMS) + Mg + O_2 + THF \rightarrow Mg[N(TMS)P(O)_2N(TMS)_2](THF)$$

$$2Mg[N(TMS)P(O)_2N(TMS)_2](THF) + MgCl_2(THF)_2 \rightarrow MgCl_2(THF)_2{\cdot}2Mg[N(TMS)P(O)_2N(TMS)_2](THF)$$

Presumably, the first reaction step occurs via chloride abstraction and electron transfer initiated by the magnesium. The rearrangement of the formed intermediate $(TMS)_2N-N(TMS)-PCl^-$ ion (**1_an**) to $(TMS)N-P-N(TMS) + Cl^-$ (**2_an**) is an exergonic process (−57.3 kcal/mol) with an estimated activation barrier of ca. 1−2 kcal/mol (**TS_an**, Table 2, Figure 6). Because of this very small barrier, a PNP species such as **2_an** can be formed easily under the described reaction conditions.

$MgCl_2(THF)_2{\cdot}2Mg[N(TMS)P(O)_2N(TMS)_2](THF)$ crystallizes in monoclinic space group $P2_1/n$ with four molecules in the unit cell (Figure 7, Table S4). Formally, **8** is composed of $2Mg[N(TMS)P(O)_2N(TMS)_2](THF)$ that is bridged by one $MgCl_2(THF)$ moiety via the two Cl^- anions. Additionally, one O atom of each $[(TMS)NP(O)_2N(TMS)]^{2-}$ dianion coordinates to the $MgCl_2(THF)$ moiety, resulting in an octahedral coordination sphere for this Mg atom (Mg3, Figure 7, Table S4). In contrast, the other two Mg atoms sit in a strongly distorted trigonal bipyramidal environment that is built from one Cl, one N (imido N), and three O ligand atoms (one O from THF and one O from both $[(TMS)NP(O)_2N(TMS)]^{2-}$ anions). The almost trigonal-planar-coordinated amino N atom (N1, N3) is not involved in the complexation at all. The amino(imido)phosphonate dianion in **8** represents a hitherto unknown dianion with phosphorus in a tetragonal environment and two significantly different P−N bond distances ($d(P_1-N_4(TMS)) = 1.594(2)$, $d(P_1-N_3(TMS)_2) = 1.681(2)$, Table S4, Figure 7). The best Lewis representation (according to NBO analysis) is displayed in Figure 8.

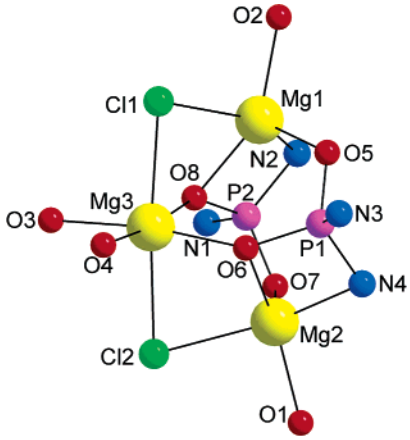

Figure 7. Cluster framework of **8**. All Si, C, and H atoms are omitted for clarity. Bond lengths [Å] and angles [deg]: P1−N3 1.681(2), P1−O5 1.526(2), P1−N4 1.594(2), P1−O6 1.550(2), P2−N1 1.686(2), P2−O7 1.521(2), P2−N2 1.589(2), P2−O8 1.553(2), N3−Si4 1.767(2), N4−Si6 1.693(2), N3−Si5 1.762(2), N4−Mg2 2.106(2), O6−Mg2 2.137(2), O6−Mg3 2.041(2), O5−Mg1 1.960(2), O7−Mg2 1.964(2), Mg2−Cl2 2.460(1), Mg3−Cl2 2.552(1), Mg1−Cl1 2.473(1), Mg3−Cl1 2.524(1), N1−P2−N2 112.1(1), O5−P1−O6 108.49(9), N3−P1−N4 113.0(1), O5−Mg1−O8 114.26(8), Cl1−Mg1−N2 147.29(7), O5−Mg1−O2 103.00(8), Cl1−Mg3−Cl2 175.01(4), O8−Mg1−N2 70.18(7), Cl2−Mg2−N4 146.78(7), O2−Mg1−O8 142.75(8).

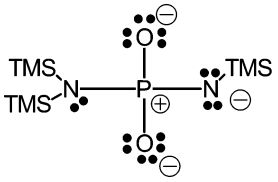

Figure 8. Best Lewis representation (according to NBO analysis) of the $[(TMS)NP(O)_2N(TMS)]^{2-}$ dianion.

In recent years, a great deal of research has been carried out involving the preparation and characterization of imido $[NR]^{2-}$ (R = H, alkyl, aryl) analogues of common oxo anions such as $[PO_4]^{3-}$.[33] The imido group is isoelectronic with the oxo $[O]^{2-}$ substituent. Replacement of one or more oxo ligands by an imido group often generates polyanions (e.g., tetra-$([P(NR)_4)]^{3-}$)[34] or diimidophosphate ions ($[R_2P(NR)_2]^{2-}$)).[35] Recently, Chivers et al. reported on the formation of tetraimidophosphate, which complexes M_2O_3 rings (M = Li, K).[36]

Computations

On the basis of the fact that **3** represents a thermally stable species at ambient temperature but slowly releases TMS−Cl at temperatures above 65 °C (in solution as well as in substances), we have carried out DFT calculation to estimate

(33) (a) Brask, J. K.; Chivers, T. *Angew. Chem., Int. Ed.* **2001**, *40*, 3960. (b) Aspinall, G. M.; Copsey, M. C.; Leedham, A. P.; Russell, C. A. *Coord. Chem. Rev.* **2002**, *227*, 217.
(34) Raithby, P. R.; Russell, C. A.; Steiner, A.; Wright, D. S. *Angew. Chem., Int. Ed. Engl.* **1997**, *36*, 649.
(35) Steiner, A.; Zacchini, S.; Richards, P. I. *Coord. Chem. Rev.* **2002**, *227*, 193.
(36) Armstrong, A.; Chivers, T.; Parvez, M.; Schatte, G.; Boere, R. T. *Inorg. Chem.* **2004**, *43*, 3453−3460.

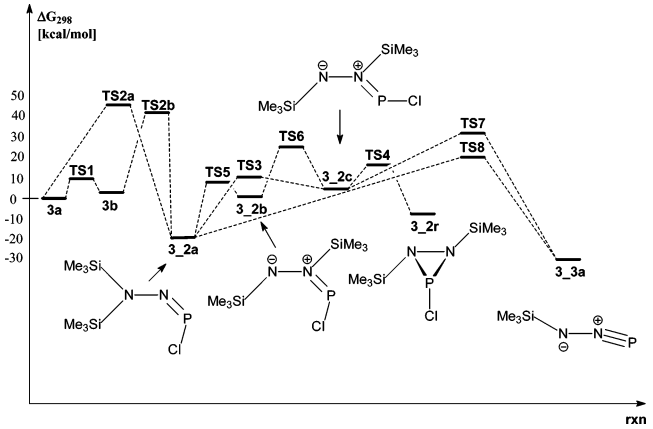

Figure 9. PES of the intrinsic TMS−Cl elimination of **3** (B3LYP/6-31G-(d,p), part I).

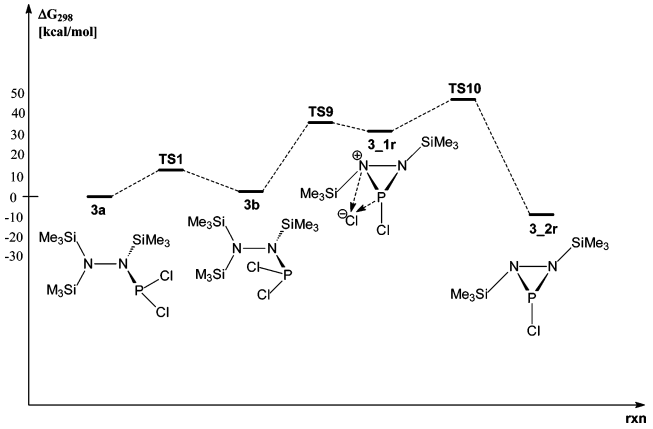

Figure 10. PES of the intrinsic TMS−Cl elimination of **3** (B3LYP/6-31G(d,p), part II).

the gas-phase activation barriers and to investigate the intrinsic reaction path resulting in the formation of (TMS)-NNP species.

Three isomers were found for **3**, of which two (**3a** and **3b**, Figure 1) are close in energy (ΔG_{298}(**3b** − **3a**) = 4 kcal/mol), whereas as ring isomer **3_1r** is about 33.5 kcal/mol less favorable (Figure 10). The energy barriers for the **3a** → **3b** and **3b** → **3_1r** isomerization reactions are about 12 kcal/mol (TS1, Table 2, Figures 9 and 10) and 31.5 kcal/mol (TS9), respectively. Formally, all three isomers of **3** are able to eliminate TMS−Cl in an unimolecular intrinsic reaction process, and *all* of these reactions represent exergonic reactions when the formation of the most stable isomer is considered (Table 2, **3a** → **3_2a**: −20.6, **3a** → **3_3a**: −33.5, **3_2a** → **3_3a**: −12.9 kcal/mol). In a ^{31}P NMR experiment, we were able to observe the TMS−Cl elimination, resulting in the formation of $(TMS)_2$NNPCl, **3_2a** (138 ppm). It is known that compounds similar to **3a**, such as $[(Me_3Si)_2N]_2PCl$, tend to liberate TMS−Cl and have to be stored at −78 °C.[3d,31] Recently, Pfister-Guillouzo et al. reported on an experimental and theoretical study of chlorosilane elimination in a photoelectron spectroscopy−flash vacuum thermolysis experiment that allowed them to synthesize the cis form of the weakly hindered chloro(imino)-phosphane Cl−P═NSiMe_2^{t}Bu starting from $(SiMe_2{}^tBu)_2N-PCl_2$.[37] Usually, phosphaimines are not easy to study experimentally because of their kinetic instability due to the high reactivity of the π_{PN} bond ([2 + 2] and [2 + 1] dimerization).

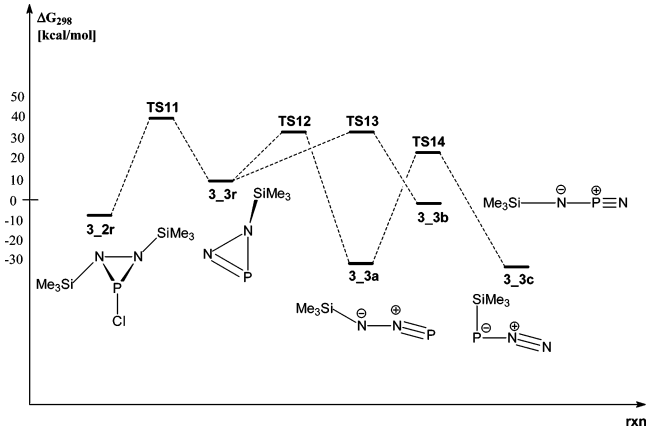

Figure 11. PES of the intrinsic TMS−Cl elimination of **3_2r** (B3LYP/6-31G(d,p), part I).

The smallest activation energy for the exothermic TMS−Cl elimination is found for **3_1r** with ca. 15 kcal/mol (TS10), resulting in stable NNP ring isomer **3_2r** (Figure 10). The energy barriers to TMS−Cl elimination for **3a** and **3b** of 45.4 and 38.8 kcal/mol are too high to be overcome by heating (TS2a, TS2b). Thermal activation may be achieved for energy barriers up to 30 kcal/mol. However, as experimentally shown, the TMS−Cl elimination is accelerated by Lewis acids such as $AlCl_3$. We assume that Lewis acids (e.g., also traces of Li^+ cations or SiO_2 surface) decrease the energy barriers for **3a** and **3b** dramatically.

The most stable $(TMS)_2$NNP−Cl isomer with an NNP moiety is bent form **3_2a** (with two TMS groups at the terminal N atom and a P═N double bond) followed by ring-shaped isomer **3_2r** with one TMS group at each N atom (ΔG_{298}(**3_2r** − **3_2a**) = 11.9 kcal/mol). Bent isomers **3_2b** and **3_2c**, also with one TMS group at each N atom, are less stable at 21.3 and 24.3 kcal/mol. All of the $(TMS)_2$NNPCl isomers are separated by activation barriers between 12 and 31 kcal/mol (ΔG_{298}(TS5) = 27.3, ΔG_{298}(TS3) = 31.2, ΔG_{298}-(TS6) = 25.0, ΔG_{298}(TS4) = 12.7 kcal/mol; Figure 9). TS5 describes the transition state of a 1.2 silyl shift. Experimentally, an activation barrier of 18.3 kcal/mol was estimated in a ^{1}H NMR experiment for a 1.3 silyl shift in (TMS)NPN-$(TMS)_2$.[2a]

Ring-shaped isomer **3_2r** can be regarded to be a diazaphosphoridin. There are two possible isomers that differ in the position of the TMS group, as displayed in Figure 12 (ΔG_{298}(**3_2r2** − **3_2r**) = 7 kcal/mol). Niecke et al. were able to generate a diazaphosphoridin in a three step synthesis: (i) metalation of $Me_3CNHNHCMe_3$ with BuLi in hexane, (ii) adding R_2NPF_2 (R = Me_2CH, Me_3Si) to give $Me_3CNHN(CMe_3)PFNR_2$, which cyclized with (iii) MeLi to a diazaphosphoridin. The diazaphosphoridin was shown to isomerize slowly at 50 °C to diiminophosphorane (valence isomer, a phosphorus−nitrogen ylide), which reacted further to give cis and trans cycloadducts (dimerization).[38] N_2

(37) Miqueu, K.; Sotiropoulos, J.-M.; Pfister-Guillouzo, G.; Romaneko, V. D. *New. J. Chem.* **2001**, *25*, 930−938.

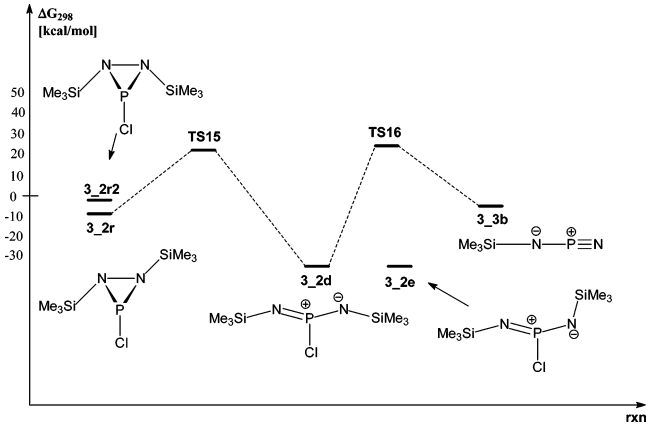

Figure 12. PES of the intrinsic TMS−Cl elimination of **3_2r** (B3LYP/6-31G(d,p), part II).

cycloelimination of λ^3-tetrazaphospholes represents another way to produce diazaphosphoridins, which was discussed by the same group.[39] In both cases, the authors describe the ring opening of the investigated λ^3-diazaphosphiridines, resulting in the formation of phosphorus−nitrogen ylide species R−N═P(R)$^+$−N(R)$^-$. Indeed, our theoretical study has been displayed in agreement with the experimental observation;[39] the ring opening of **3_2r** is an exergonic process with an estimated activation barrier of 32.0 kcal/mol (Figure 12, TS15) and an energy gain of 25.7 kcal/mol. Moreover, the formed phosphorus−nitrogen ylide **3_2d** is more thermodynamically stable than **3_2a** by 13.8 kcal/mol. In addition to **3_2d** with two TMS groups in cis position with respect to the P−Cl bond, we were able to locate another isomer **3_2e** with one TMS group in the cis and the second in the trans position (Figure 12). Additionally, several rotamers were found to be close in energy (ΔG_{298} < 0.4 kcal/mol). Interestingly, both isomers represent planar species along the Si−N−P−N−Si moiety including the Cl atom and are very close in energy (ΔG < 1 kcal/mol).

The intrinsic elimination steps of another TMS−Cl molecule starting from **3_2a**, **3_2c** or **3_2r**, and **3_2d** are calculated to possess large activation barriers to the formation of TMS−NNP isomers of 28.7 (TS7), 40.4 (TS8), 48.8 (TS11), and 59.3 kcal/mol (TS16). The β elimination of TMS−Cl from the two open-chain bent isomers (**3_2a** and **3_2c)** results in the formation of the trans bent TMS−N−N−P azide analogue (**3_3a)** with energy gains of 10.6 and 35.1 kcal/mol, respectively (Figure 9). In contrast to **3_2a** and **3_2c**, a ring-shaped isomer (**3_3r)** is obtained upon TMS−Cl elimination in **3_2r** in an endergonic reaction. The ring opening of the ring-shaped isomer (**3_3r)** represents an exergonic reaction yielding either trans bent isomer **3_3a** or linear **3_3b** with N−P−N−TMS connectivity. The activation barriers to overcome are 21.3 (TS12) and 21.2 (TS13) kcal/mol. It is interesting that the isomer that is the most stable thermodynamically has the TMS group attached to the phosphorus atom in TMS−PNN (**3_3c)** (relative energy values **3_3c**: 0.0, **3_3a**: 2.1, **3_3b**: 29.7 kcal/mol). Formally, **3_3c** can be obtained in a rather unlikely process of a 1.3 sigmatropic TMS shift in **3_3a** with a very large activation barrier of 52.6 kcal/mol (TS14).

Experimentally, it should be very difficult to isolate species of the **3_3a**−**3_3c** type because they are expected to undergo cyclization reactions ([2 + 2], [2 + 3], etc.) to form PN oligomeres. Additionally, cyclization reactions and oligomer formation are already expected from the starting materials leading to **3_3a**−**3_3c**. Only the use of very large bulky groups may stabilize the low-coordination number kinetically at the phosphorus atom in the phosphorus analogues of the covalent azide.

Structure and Bonding of the (TMS)NNP Species. Both the **3_3a** and **3_3c** species show a trans bent structure similar to the structure of covalent azides, whereas isomer **3_3b** possesses a linear arrangement of the Si−N−P−N moiety (Figure 11).[40] According to NBO analysis, the phosphorus atom in **3_3b** is almost sp hybridized with no lone pair; in isomers **3_3a** and **3_3c**, a lone pair with more than 80% s character is localized. This may explain why isomer **3_3b** is less favored energetically by ca. 30 kcal/mol. The s-type lone pair in the **3_3c** species and the p-type atomic orbital building the NBO of the Si−P bond are mainly responsible for the small 93° N−P−Si angle, whereas the sp^2-hybridized N atom in **3_3a** accounts for the 129° N−N−Si angle. The Si−N and N−P bonds are strongly polarized (see partial net charges in Table S6). According to the partial charges, the P−N bond in **3_3c** seems to be less polarized because of the charge transfer from the TMS group attached to the P atom;[41] however, an inspection of the NBO describing the σ PN bond displays the typical degree of polarization of ca. 80% (N) to 20% (P), as found for all investigated PN species. Interestingly, NBO analysis displays a different degree of polarization for the σ (e.g., in **3_3a** N: 76% vs P: 24%) compared to the π PN bonds (N: 66 and 56% vs P: 34 and 44%). The Si−N bonds also represent highly ionic bonds with ca. 84% localization at the N atom (for **3_3a**, **3_3b**, and **3_3r**), whereas the almost covalent Si−P bond in **3_3c** is localized at only 38% at the P atom. (A pure covalent bond corresponds to 50% localization at each center of a two-center bond.)

As expected, the N−N distances decrease upon TMS−Cl elimination as long as a chainlike structure is formed (**3a**: 1.466, **3_2a**: 1.333, **3_3a**: 1.218, **3_3c**: 1.137, and cf. **3_3r**: 1.385 Å). In the ring-shaped isomers (**3_1r**, **3_2r**, and **3_3r)**, rather long N−N and P−N distances are found because of ring strain. The shortest N−N bond length is found in TMS−PNN (**3_2c**), with 1.137 Å (cf. d_{calcd}(NN, N_2) = 1.105 Å[42]). Interestingly, the shortest P−N distances are found in TMS−N═P═N (**3_3b**) with 1.502 and 1.505 Å. In contrast, the P−N bond lengths of **3_2a** (with a formal

(38) Niecke, E.; Schwichtenhoevel, K.; Schaefer, H. G.; Krebs, B. *Angew. Chem.* **1981**, *93*, 1033−1034. Niecke, E.; Schwichtenhoevel, K.; Schaefer, H. G.; Krebs, B. *Angew. Chem., Int. Ed. Engl.* **1981**, *11*, 963−964.
(39) Niecke, E.; Schäfer, H.-G.*Chem. Ber.* **1982**, *115*, 185−200.
(40) Schulz, A.; Tornieporth-Oetting, I. C.; Klapötke, T. M. *Inorg. Chem.* **1994**, *34*, 4343.
(41) Barlos, K.; Hübler, G.; Nöth, H.; Wanninger, P.; Wiber, N.; Wrackmeyer, B. *J. Magn. Reson.* **1978**, *31*, 363−376.
(42) Calculated at B3LYP/6-31G(d,p); cf. d_{exp} = 1.0976 Å.

PN double bond) and **3_3a** (with a formal PN bond order > 2) are fairly similar with 1.543 and 1.544 Å but elongated by 0.04 Å compared to that of **3_3b**. In **3_2a**, the fairly short P−N bond can be explained by the intramolecular donor−acceptor interaction of the p-LP at the adjacent N atom with the σ^*(P−Cl) orbital similar to that in **3a** or **3b**, which is not possible in **3_3a** (Figures 9, 11).

Conclusions

The reactions of diphenyl(chloro)phosphane and phenyl-(dichloro)phosphane with bis[lithium-tris(trimethylsilyl)-hydrazide] represent a fast and clean reaction resulting in the formation of hydrazinophosphanes **1** and **2** in high yields. Both species possess fairly small P−N bond lengths due to intramolecular donor−acceptor interactions and represent thermally stable (with respect to TMS−Cl elimination) compounds. Hence, **1** and **2** represent ideal precursors for further synthesis of compounds containing a NNP unit. Reaction with sulfur or selenium results in the formation of the oxidation products **4**−**7**. Thermodynamic stabilization of the chlorine-containing systems appears in the important interaction between the nitrogen lone pair and the antibonding P−Cl σ^* orbital.[37]

All three steps of the reaction of bis[lithium-tris(trimethylsilyl)-hydrazide] with phosphorus trichloride represent exothermic reactions. Large activation barriers are responsible for the thermal stability of **3a** ($(TMS)_2N(TMS)PCl_2$), linear **3_2a** ($(TMS)_2NNP-Cl$), and cyclic **3_2r** with respect to intramolecular TMS−Cl elimination. Investigation of the potential energy surface of (TMS)NNP revealed that **3_3c** (TMS−PNN) represents the global minimum. The analysis of the chemical bonds using the NBO partitioning scheme shows a strong polarization of the N−P and N−Si bonds.

Acknowledgment. A.S. thanks Professor Dr. T. M. Klapötke (LMU München) for his generous support and advice. We also thank the Leibniz Rechenzentrum for a generous allocation of CPU time. We are indebted to Dr. K. Karaghiosoff and Professor Dr. A. Schmidpeter for helpful advice and Dr. M. Suter for measuring an X-ray data set.

Supporting Information Available: Experimental details for the synthesis of the oxidized compounds ($(TMS)_2N-(TMS)N-P(S)Ph_2$ (**4**), $(TMS)_2N-(TMS)N-P(Se)Ph_2$ (**5**), $(TMS)_2N-(TMS)N-P(S)Ph(Cl)$ (**6**), $(TMS)_2N-(TMS)N-P(Se)Ph(Cl)$ (**7**)). X-ray crystallographic files in CIF format for the structure determinations of **1**, **2**, **4**, and **8** and the calculated structural data, energies, IRCs, and frequency data of all of the investigated species (archive entries). This material is available free of charge via the Internet at http://pubs.acs.org or from the author.

IC048286M